2D Materials

PAPER • OPEN ACCESS

Strain induced lifting of the charged exciton degeneracy in monolayer MoS_2 on a GaAs nanomembrane

To cite this article: Jakub Jasiski *et al* 2022 *2D Mater.* **9** 045006

2D Materials

CrossMark

OPEN ACCESS

RECEIVED
20 April 2022

REVISED
18 June 2022

ACCEPTED FOR PUBLICATION
27 June 2022

PUBLISHED
7 July 2022

PAPER

Strain induced lifting of the charged exciton degeneracy in monolayer MoS_2 on a GaAs nanomembrane

Jakub Jasiński[1,2], Akshay Balgarkashi[3], Valerio Piazza[3], Didem Dede[3], Alessandro Surrente[1], Michał Baranowski[1], Duncan K Maude[2], Mitali Banerjee[4], Riccardo Frisenda[5,6], Andres Castellanos-Gomez[5], Anna Fontcuberta i Morral[3] and Paulina Plochocka[1,2,*]

[1] Department of Experimental Physics, Faculty of Fundamental Problems of Technology, Wroclaw University of Science and Technology, 50-370 Wroclaw, Poland
[2] Laboratoire National des Champs Magnétiques Intenses, EMFL, CNRS UPR 3228, Université Grenoble Alpes, Université Toulouse, Université Toulouse 3, INSA-T, Grenoble and Toulouse, France
[3] Laboratory of Semiconductor Materials, Institute of Materials, École Polytechnique Fédérale de Lausanne, 1015 Lausanne, Switzerland
[4] Laboratory of Quantum Physics, Topology and Correlations, Institute of Physics, École Polytechnique Fédérale de Lausanne, 1015 Lausanne, Switzerland
[5] Materials Science Factory, Instituto de Ciencia de Materiales de Madrid (ICMM-CSIC), Madrid E-28049, Spain
[6] Physics Department, Sapienza University of Rome, 00185 Rome, Italy
[*] Author to whom any correspondence should be addressed.

E-mail: paulina.plochocka@lncmi.cnrs.fr

Keywords: nanomembranes, transition metal dichalcogenides, heterostructures, gallium arsenide

Supplementary material for this article is available online

Abstract

Strain is a commonly used tool to tune the optoelectronic properties of semiconductors. It is especially effective for transition metal dichalcogenides (TMDs), which can withstand extreme strain up to 10%. To date, localised strain fields have been applied by transferring TMDs flakes onto a patterned SiO_2 substrate. Here, we present a novel approach, where the strain in MoS_2 monolayer is induced by an array of homoepitaxially grown GaAs nanomembranes. This represents a first step towards the integration of TMD monolayers with III–V semiconductor nanostructures, which is essential to develop scalable nanophotonic platforms. The strain imposed by the nanomembrane lifts the degeneracy of the exciton states, leading to linearly polarised emission. The principal axis of the linear polarisation of the emission is strictly determined by the orientation of the nanomembranes. This result is fully consistent with the expected broken crystal symmetry resulting from the imposed uniaxial strain.

Among the plethora of techniques used to tailor the electronic properties of semiconductors, the application of external stresses has been particularly successful [1]. Strain engineering is exceptionally attractive for two-dimensional (2D) layered materials, which possess an excellent mechanical robustness and flexibility [2]. For instance, transition metal dichalcogenide (TMD) monolayers can withstand strains as high as 10% before breaking [3]. Strain profoundly affects the properties of these materials, and can be used to control their band structure [4–8] and vibrational properties [5, 8–11]. Strain in 2D materials naturally occurs during the deposition process [4]. Unlike this random strain distribution, a controllable spatial strain variation can be imposed by using an appropriately patterned substrate [12–15]. This can serve to induce carrier or exciton funnelling caused by inhomogeneous strain fields [16–19] or the deterministic positioning of single photon emitters [12, 13, 20]. Strain also breaks the symmetry of the TMD crystal, which lifts the degeneracy of the excitonic states, and changes the selection rules of the optical transitions [14, 15, 21–25].

To date, localized TMD stressors have consisted mainly of patterned SiO_2 and SiN substrates [12, 13, 20]. These materials, however, are plagued by dangling bonds and trapped charges. These perturb the electrostatic environment of the TMD layer, which is detrimental for the device functionality [26]. An attractive alternative for the strain engineering of the optoelectronic properties of TMDs is represented by III–V-based epitaxially grown nanostructures

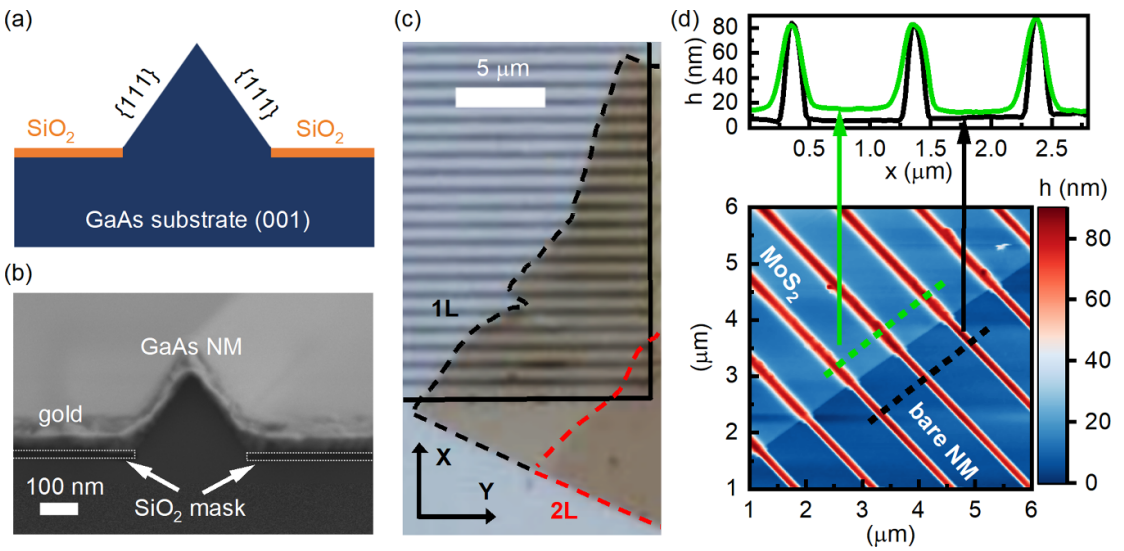

Figure 1. (a) Schematic of a GaAs nanomembrane cross section. (b) Scanning electron microscope (SEM) image of a GaAs nanomembrane cross section with a 100 nm scale bar. A gold layer (not present on the investigated sample) was deposited on the nanomembrane with the purpose of improving the contrast of the SEM image. (c) Micrograph of the sample with 5 μm scale bar. The horizontal dark lines are the GaAs nanomembranes. The MoS_2 flake lies partially on the nanomembrane region ($X > 0$) and partially on the bare substrate ($X < 0$). 1L and 2L denote monolayer and bilayer regions of the MoS_2 flake. (d) Bottom: AFM image of MoS_2 flake around the flake edge showing areas of bare nanomembranes ('bare NM') and with deposited flake ('MoS_2'). The area of the image is marked in supplementary figure 1(a). Top: AFM profiles across bare nanomembranes (black) and with deposited flake (red).

[27]. The absence of trapped surface charges is expected to reduce the line width and improve the stability of the optical spectra [28, 29]. Moreover, III–V semiconductors are considered essential building blocks for monolithically [30] or heterogeneously [31] integrated quantum photonic circuits. The integration of monolayer TMDs on III–V semiconductors can potentially lead to their use in scalable nanophotonic platforms.

Uniaxial strain has already been used to induce linear dichroism in MoS_2 monolayers [32]. However, a thorough investigation of the effects of uniaxial strain on the linear polarisation behaviour of excitonic complexes is currently lacking. Here, we demonstrate that the application of uniaxial strain leads to a linear polarisation of the charged exciton emission in MoS_2 monolayers. We induce strain by transferring a MoS_2 monolayer onto GaAs nanomembranes grown by selective area epitaxy, which allows to achieve an excellent control over the crystal quality, morphology, size and position of the resulting nanostructures [33–37]. Atomic force microscopy (AFM) demonstrates that the transferred monolayer conforms to the morphology of the nanomembranes. We correlate the presence of strain, deduced from structural and morphological data obtained by AFM, with the spatial dependence of the Raman and photoluminescence (PL) spectra. The anisotropic potential introduced by the uniaxial strain leads to the formation of excitonic states with dipole moments oriented parallel and perpendicular to the strain axis, as observed in single photon emitters hosted in WSe_2 monolayers [14, 15]. We make use of the uniaxial strain induced by the nanomembranes to demonstrate for the first time a control over the linear polarisation of charged exciton emission in MoS_2.

The substrate consists of an array of 20 μm long, nominally $\simeq$50 nm wide GaAs nanomembranes, grown by selective area epitaxy with a 1 μm pitch. The flat areas of the GaAs substrate between the nanomembranes are covered by a 25 nm thick SiO_2 layer, used as the mask during the growth process (see section 1 for additional details on the growth and fabrication of the sample). Schematic and scanning electron microscope (SEM) images of a cross sectional view of a single nanomembrane are shown in figures 1(a) and (b). The deposited MoS_2 flake comprises monolayer (1L) and bilayer (2L) regions, which can be distinguished from both optical contrast and Raman spectra. These regions are indicated by black and red dashed lines in the micrograph displayed in figure 1(c). In the topmost part of figure 1(d), we show AFM profiles extracted in the direction perpendicular to the axis of the nanomembranes from both an area on the flake and the bare nanomembranes (see figure 1(d), bottom panel for the full AFM scan). The flake creates a tent-like structure on the nanomembranes, while between them it is suspended above the substrate by $\sim$10 nm, as suggested by the offset baselines of the profiles of figure 1(d).

We use optical spectroscopy to gain insight into the strain distribution across the MoS_2 flake. Representative Raman and PL spectra from regions without (1) and with (2) nanomembranes are shown in figures 2(a) and (b). Both give information

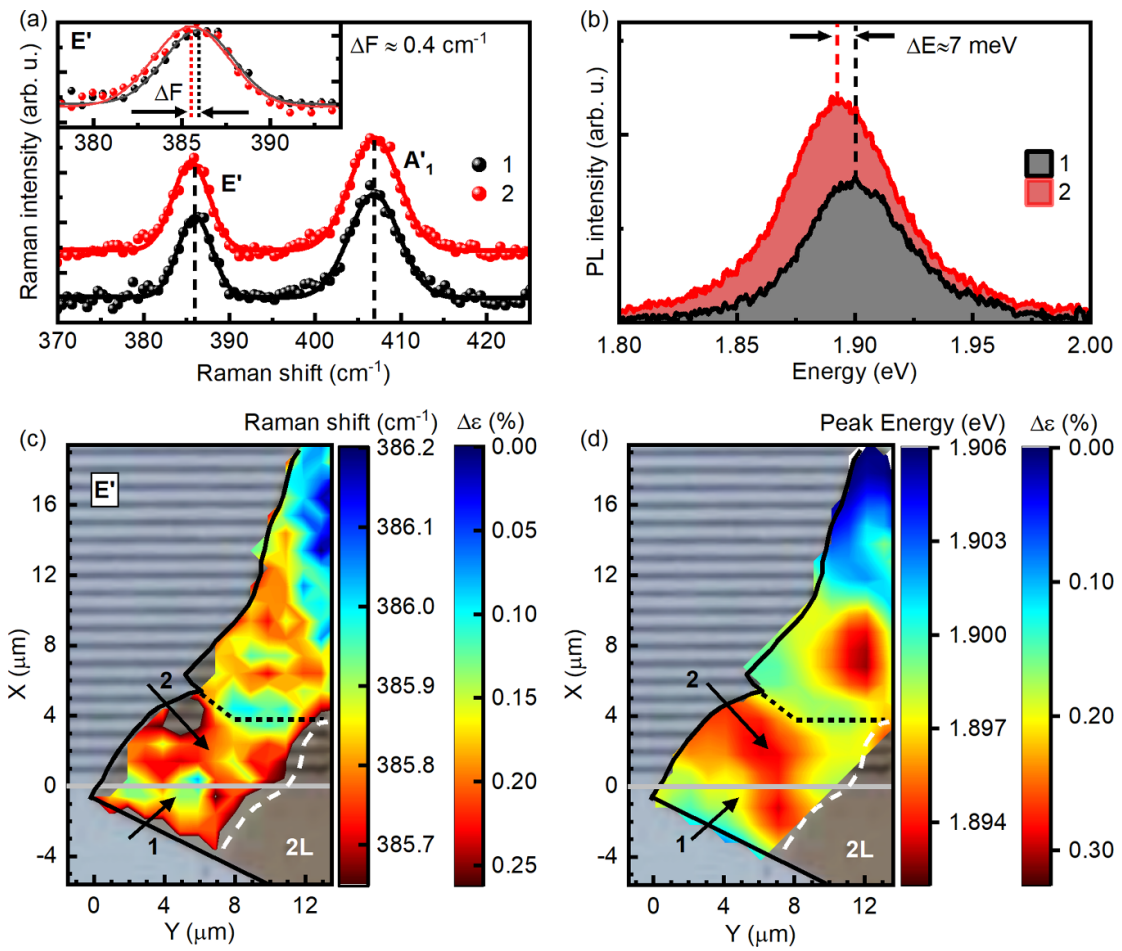

Figure 2. (a) Main: low temperature ($T = 4$ K) MoS_2 Raman spectra (E' and A_1' modes) from regions of the flake on the flat substrate (1) and on nanomembranes (2). The spectra are vertically shifted for clarity. The solid lines are double-Gaussian fits to the data. The inset shows an expanded view of the E' mode measured in regions (1) and (2). (b) Representative low temperature ($T = 4$ K) PL spectra from regions (1) and (2). The PL and Raman spectra do not correspond to the points where the largest shift is measured. (c) E' Raman mode frequency map derived from Gaussian fitting. The second colour scale indicates the strain $\Delta\varepsilon$ derived from the E' mode frequency based on [38]. (d) PL peak energy map derived from Lorentzian fitting. The black dashed line in panels (c, d). Contour of the broken MoS_2 flake. The second colour scale indicates the strain $\Delta\varepsilon$ derived from the charged exciton PL peak energy based on [38].

concerning the imposed strain, since the E' Raman mode (at $\sim$386 cm^{-1}) and the PL peak energy red shift when the TMD monolayer is subjected to tensile strain [5, 9–11, 38]. Across the investigated area, the E' frequency shifts by $\simeq$0.6 cm^{-1} from 386.2 to 385.6 cm^{-1}, which translates to $\simeq$0.3% of tensile strain [38]. The PL peak energy shifts by $\sim$13 meV from 1.907 to 1.893 eV. The PL spectrum is always dominated by the trion emission (X_T), and only in a few regions is a high energy shoulder around 1.94 eV observed, which we attribute to the A exciton (X_A) transition (see supplementary information). The strong preference for trion formation can be explained by the charge transfer from the GaAs/SiO_2 substrate or GaAs nanomembranes [28, 39].

In figures 2(c) and (d), we plot the position dependence of the E' peak frequency and the PL peak energy. The strain (second colour scale shows strain calculated from Raman shift [38]) can be directly estimated from the Raman map, which confirms the deterministic impact of the nanomembranes on the strain in MoS_2 layer. In general, in the nanomembrane regions we observe places where the tensile strain is increased compared to regions without nanomembranes. This manifests as a softening of the E' mode and a red shift of the PL spectrum, which are visible as red and yellow parts of the maps of figures 2(c) and (d). The E' mode is also softened at the border between mono- and bilayer, which we attribute to the convolution of the signals from both areas (E' mode is softer in bilayer than in monolayer [40]). It is worth noting that some strain can also appear due to lateral interface between mono- and bilayer part [41]. The variation of strain on the monolayer reference flake (supplementary figure 6(b)) is three times lower than in the investigated sample, and it also shows no rapid changes as in the case of monolayer deposited on the nanomembranes. Therefore, these spatially resolved measurements confirm that strain can be successfully

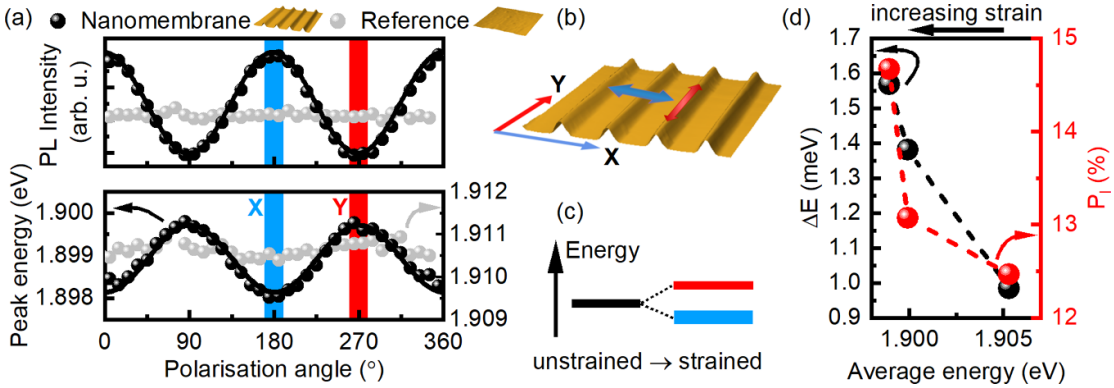

Figure 3. Low temperature ($T = 4$ K) polarisation resolved PL. (a) Comparison of polarisation angle dependence of PL intensity and energy between reference flake and flake deposited on the nanomembranes. (b) Schematic of MoS_2 deposited on a nanomembranes. The blue and red arrows denote the dipoles across (X) and (Y) along nanomembranes, respectively. (c) Schematic depiction of exciton states, showing degeneracy lifting along X and Y directions due to uniaxial strain. (d) Correlation between average emission energy and observed degree of linear polarisation (DOLP) and energy splitting ΔE from 3 measurements on different regions of the MoS_2 flake on the nanomembranes.

applied using GaAs nanomembranes. Unfortunately, the strain pattern deduced from the Raman and PL maps does not reproduce exactly the pattern of the nanomembranes. Our setup has a finite spatial resolution. This implies that the strain pattern reported in figures 2(c) and (d) is actually convoluted with a Gaussian instrument response function having a standard deviation of ~600 nm, which is close to the period of the nanomembrane array. This, together with the unavoidable folding, wrinkling and cleaving of the monolayer during the transfer, prevents from the observation of a strictly periodic pattern similar to that of nanomembranes. For example, in areas where the MoS_2 flake is broken, as revealed by AFM measurements shown in the supplementary information and highlighted by the dashed black line in figures 2(c) and (d), we observe a hardening of the E' mode accompanied by a blue shift of the PL spectrum, which indicates that the strain is partially relaxed despite the presence of nanomembranes.

To explore the effects of the strain on the PL response more in detail, we measure linear polarisation-resolved PL at various positions on the nanomembranes, and on a separate, flat flake lying well away from the nanomembranes region (denoted as Reference flake). Figure 3(a) shows the PL intensity and energy of the charged exciton as a function of the polarisation detection angle. Both intensity and energy of the peak show a sinusoidal dependence on the polarisation angle when the PL is collected from the flake on the nanomembrane, while they do not for the reference flake. From the polarisation angle dependence of the intensity, we estimate the degree of linear polarisation (DOLP) as:

$$P_l = \frac{I_{max} - I_{min}}{I_{max} + I_{min}},$$

where I_{max} and I_{min} are the maximal/minimal emission intensity, respectively. For the MoS_2 flake on the nanomembrane, we consistently observe DOLP in the range of ≃10%–15% with higher PL intensity for the polarisation in the direction perpendicular to the nanomembrane. The change in the PL intensity is accompanied by an energy shift of ≃1–2 meV between the two orthogonal polarisations (see figure 3(a), lower panel). This behaviour reflects the degeneracy lifting of the two in-plane states, related to K and K' valleys [22], due to the presence of uniaxial strain. The two transitions are linearly polarised with dipole moments of the lower (upper) energy transitions aligned perpendicular (parallel) to the nanomembrane direction, as shown schematically in figures 3(b) and (c). The thermal distribution of charged excitons leads to a higher PL intensity for the lower energy of emission, and induces a non zero DOLP. However, the measured DOLP is significantly smaller than ≃90%, which is the value expected at 4 K for states separated by ~1.5 meV, assuming a Boltzmann distribution of the populations. The observed DOLP ≃ 15% is consistent with a temperature $T \simeq 55$ K, which suggests that the charged excitons do not have time to thermalize before recombining due to the short PL lifetime in monolayer TMDs [42]. The role of the strain in the induced DOLP is further corroborated by the fact that the DOLP and energy splitting both increase with increasing strain (red shift of PL), as we show in figure 3(d).

The behaviour of the PL spectrum in strained TMDs observed here resembles that of quantum dots, where a symmetry breaking by uniaxial strain or confinement lifts the degeneracy of excitonic states, which changes the polarisation the PL from circular to linear [43]. Similarly, in the case of TMDs, it is expected that uniaxial strain breaks the three-fold rotational symmetry of the lattice, resulting in a non-zero intervalley exchange interaction. This effectively acts as an in-plane Zeeman field on the valley pseudospin,

which splits and mixes K and K′ states leading to linearly polarised emission [21, 22]. Recently, a splitting of both trion and exciton states has been observed in randomly uniaxially-strained WSe_2 monolayers [44]. Here, we have shown that this can be deterministically controlled by using an appropriate substrate design.

To summarise, we have shown that MoS_2 monolayers can be successfully transferred onto patterned III–V substrates, in particular GaAs nanomembranes. We have demonstrated how the uniaxial strain imposed by the nanomembranes affects the optical properties of monolayer MoS_2. The uniaxial strain results in linearly polarised PL (DOLP $\simeq$ 10%–15%) and in an energy splitting of $\simeq$1–2 meV. This is fully consistent with the expected degeneracy lifting of the fine structure of excitonic states in the K and K′ valleys, due to the strain-induced breaking of the in-plane crystal symmetry. This is a promising step for the use of TMDs in applications that necessitate the use of linearly polarised light. Selective area epitaxy can therefore be used as a deterministic strain-engineering method that would remove the need for external strain control such as piezoelectric substrates or mechanical bending.

1. Methods

1.1. Optical spectroscopy

For low temperature measurements, the samples are mounted on the cold finger of a helium flow cryostat. The cryostat is bolted to computer controlled, motorised *XY* translation stages, which allow for two-dimensional in-plane motion. The position of the stages is controlled with micrometer screws, either manually or using automated stepper motors. The motors allow for mapping measurements, by scanning the sample surface step by step. The PL and Raman measurements were performed using CW solid state lasers emitting either at 405 or 532 nm. The excitation beam was focused onto the sample using a 50× microscope objective with a numerical aperture of 0.55, giving a spot size of $\simeq$1 μm. For PL mapping, the signal was detected in a confocal configuration to improve the spatial resolution. The emitted PL and Raman signal or the reflected white light were collected through the same objective and redirected to a spectrometer equipped with a liquid nitrogen-cooled charge-coupled device camera. Polarisation resolved PL was achieved by the inclusion of a linear polariser and a superachromatic half-wave plate in the detection path. The polariser was set at a fixed angle in front of the spectrometer to avoid the grating polarisation-dependent efficiency, while the half-wave plate was used to rotate the detected polarisation angle.

1.2. MBE growth

Undoped GaAs (001) substrates were prepared by first depositing 25 nm of SiO_2 mask by the plasma enhanced chemical vapour deposition (PECVD). Arrays of parallel slits along the ⟨110⟩ and ⟨100⟩ directions were patterned by e-beam lithography using ZEP resist and subsequent development with low-temperature n-amyl acetate. The pattern was transferred on the SiO_2 mask by dry etching with fluorine chemistry to expose the GaAs surface in the patterned slits. A final wet etch in a dilute buffered HF solution was used to remove residual oxide layers and to reduce the GaAs surface roughness. This yielded openings varying from 30 to 100 nm in width and 10–20 μm in length, depending on the e-beam pattern. The patterned substrates were loaded in a DCA P600 Gen II molecular beam epitaxy system equipped with group III and group V solid sources. Prior to the growth, the substrates were annealed at 630 °C under As_4 flux for 10 min. The GaAs nanomembranes were grown at a temperature of 630 °C, at a Ga deposition rate of 0.3 Å s^{-1} and an As_4 partial pressure of 4×10^{-6} BEP.

1.3. Flake transfer

MoS_2 flakes were obtained by mechanical exfoliation from a natural molybdenite crystal from Moly Hill mine (Québec, Canada) on a Gel-Film (WF X4 6.0 mil) supplied by Gel-Pak. A monolayer MoS_2 flake was deterministically transferred to a nanomembrane array using an all-dry viscoelastic stamping process [45]. The flake exfoliated on a Gel-Film film is attached to a glass slide and the glass slide is used as a stamp. The stamp is first aligned with the nanomembrane array and then brought in contact using a *Z*-axis manipulation stage. Following this, a cotton bud is used to gently press the Gel-Film stamp onto the array. The stamp is gently released to transfer the flake from the Gel-Film stamp onto the nanomembrane array.

Data availability statement

The data that support the findings of this study are available upon reasonable request from the authors.

Acknowledgments

This work has been partially funded by National Science Centre Poland within the SONATA BIS program (Grant No. 2020/38/E/ST3/00194) and PRELUDIUM BIS (Grant No. 2019/35/O/ST3/02162). The Polish participation in European Magnetic Field Laboratory (EMFL) is supported by the DIR/WK/2018/07 Grant from the Ministry of Science and Higher Education, Poland. This study has been partially supported through the EUR Grant NanoX No. ANR-17-EURE-0009 in the framework of the 'Programme des Investissements d'Avenir'. This work received funding from the European Research Council (ERC) under the European Union's Horizon 2020 research and innovation program (Grant Agreement No. 755655, ERC-StG 2017 Project 2D-TOPSENSE), the Spanish Ministry of Science and Innovation

through the Project PID2020-115566RB-I00, the EU FLAG-ERA Project To2Dox (JTC-2019-009) and the Comunidad de Madrid through the Project CAIRO-CM (Y2020/NMT-6661). Authors from EPFL thank funding from SNSF via Project 196948 and acknowledge funding through the NCCR QSIT. This work has also received funding from the European Union's Horizon 2020 research and innovation programme under the Marie Skłodowska–Curie Grant Agreement No. 765075, Project LIMQUET. V P acknowledges the support by Piaget through the Scientific Award. ACG and PP acknowledge funding from the European Union's Horizon 2020 research andinnovation program under grant agreement 956813 (2Exciting),

ORCID iDs

Akshay Balgarkashi https://orcid.org/0000-0003-0504-5542
Didem Dede https://orcid.org/0000-0002-9158-8764
Alessandro Surrente https://orcid.org/0000-0003-4078-4965
Michał Baranowski https://orcid.org/0000-0002-5974-0850
Riccardo Frisenda https://orcid.org/0000-0003-1728-7354
Andres Castellanos-Gomez https://orcid.org/0000-0002-3384-3405
Anna Fontcuberta i Morral https://orcid.org/0000-0002-5070-2196
Paulina Plochocka https://orcid.org/0000-0002-4019-6138

References

[1] Trotta R, Martín-Sánchez J, Daruka I, Ortix C and Rastelli A 2015 Energy-tunable sources of entangled photons: a viable concept for solid-state-based quantum relays *Phys. Rev. Lett.* **114** 150502
[2] Lee C, Wei X, Kysar J W and Hone J 2008 Measurement of the elastic properties and intrinsic strength of monolayer graphene *Science* **321** 385–8
[3] Bertolazzi S, Brivio J and Kis A 2011 Stretching and breaking of ultrathin MoS_2 *ACS Nano* **5** 9703–9
[4] Castellanos-Gomez A, Roldán R, Cappelluti E, Buscema M, Guinea F, van der Zant H S and Steele G A 2013 Local strain engineering in atomically thin MoS_2 *Nano Lett.* **13** 5361–6
[5] Conley H J, Wang B, Ziegler J I, Haglund R F Jr, Pantelides S T and Bolotin K I 2013 Bandgap engineering of strained monolayer and bilayer MoS_2 *Nano Lett.* **13** 3626–30
[6] Zhu C *et al* 2013 Strain tuning of optical emission energy and polarization in monolayer and bilayer MoS_2 *Phys. Rev.* B **88** 121301
[7] He K, Poole C, Mak K F and Shan J 2013 Experimental demonstration of continuous electronic structure tuning via strain in atomically thin MoS_2 *Nano Lett.* **13** 2931–6
[8] Lloyd D, Liu X, Christopher J W, Cantley L, Wadehra A, Kim B L, Goldberg B B, Swan A K and Bunch J S 2016 Band gap engineering with ultralarge biaxial strains in suspended monolayer MoS_2 *Nano Lett.* **16** 5836–41
[9] Wang Y, Cong C, Qiu C and Yu T 2013 Raman spectroscopy study of lattice vibration and crystallographic orientation of monolayer MoS_2 under uniaxial strain *Small* **9** 2857–61
[10] Lee J-U, Woo S, Park J, Park H C, Son Y-W and Cheong H 2017 Strain-shear coupling in bilayer MoS_2 *Nat. Commun.* **8** 1370
[11] Doratotaj D, Simpson J R and Yan J-A 2016 Probing the uniaxial strains in MoS_2 using polarized Raman spectroscopy: a first-principles study *Phys. Rev.* B **93** 075401
[12] Palacios-Berraquero C, Kara D M, Montblanch A R-P, Barbone M, Latawiec P, Yoon D, Ott A K, Loncar M, Ferrari A C and Atatüre M 2017 Large-scale quantum-emitter arrays in atomically thin semiconductors *Nat. Commun.* **8** 15093
[13] Branny A, Kumar S, Proux R and Gerardot B D 2017 Deterministic strain-induced arrays of quantum emitters in a two-dimensional semiconductor *Nat. Commun.* **8** 15053
[14] Wang Q, Maisch J, Tang F, Zhao D, Yang S, Joos R, Portalupi S L, Michler P and Smet J H 2021 Highly polarized single photons from strain-induced quasi-1D localized excitons in WSe_2 *Nano Lett.* **21** 7175–82
[15] So J-P *et al* 2021 Polarization control of deterministic single-photon emitters in monolayer WSe_2 *Nano Lett.* **21** 1546–54
[16] Feng J, Qian X, Huang C-W and Li J 2012 Strain-engineered artificial atom as a broad-spectrum solar energy funnel *Nat. Photon.* **6** 866–72
[17] Moon H, Grosso G, Chakraborty C, Peng C, Taniguchi T, Watanabe K and Englund D 2020 Dynamic exciton funneling by local strain control in a monolayer semiconductor *Nano Lett.* **20** 6791–7
[18] Lee J, Yun S J, Seo C, Cho K, Kim T S, An G H, Kang K, Lee H S and Kim J 2021 Switchable, tunable and directable exciton funneling in periodically wrinkled WS_2 *Nano Lett.* **21** 43–50
[19] Harats M G, Kirchhof J N, Qiao M, Greben K and Bolotin K I 2020 Dynamics and efficient conversion of excitons to trions in non-uniformly strained monolayer WS_2 *Nat. Photon.* **14** 324–9
[20] Kumar S, Kaczmarczyk A and Gerardot B D 2015 Strain-induced spatial and spectral isolation of quantum emitters in mono-and bilayer WSe_2 *Nano Lett.* **15** 7567–73
[21] Yu H, Liu G-B, Gong P, Xu X and Yao W 2014 Dirac cones and Dirac saddle points of bright excitons in monolayer transition metal dichalcogenides *Nat. Commun.* **5** 3876
[22] Yu H, Cui X, Xu X and Yao W 2015 Valley excitons in two-dimensional semiconductors *Natl Sci. Rev.* **2** 57–70
[23] Feierabend M, Morlet A, Berghäuser G and Malic E 2017 Impact of strain on the optical fingerprint of monolayer transition-metal dichalcogenides *Phys. Rev.* B **96** 045425
[24] Korkmaz Y A, Bulutay C and Sevik C 2021 $\mathbf{k}\cdot\mathbf{p}$ parametrization and linear and circular dichroism in strained monolayer (Janus) transition metal dichalcogenides from first-principles *J. Phys. Chem.* C **125** 7439–50
[25] Aas S and Bulutay C 2018 Strain dependence of photoluminescence and circular dichroism in transition metal dichalcogenides: a $k\cdot p$ analysis *Opt. Express* **26** 28672–81
[26] Koperski M, Nogajewski K, Arora A, Cherkez V, Mallet P, Veuillen J-Y, Marcus J, Kossacki P and Potemski M 2015 Single photon emitters in exfoliated WSe_2 structures *Nat. Nanotechnol.* **10** 503–6
[27] Roldán R, Castellanos-Gomez A, Cappelluti E and Guinea F 2015 Strain engineering in semiconducting two-dimensional crystals *J. Phys.: Condens. Matter* **27** 313201
[28] Iff O, He Y-M, Lundt N, Stoll S, Baumann V, Höfling S and Schneider C 2017 Substrate engineering for high-quality emission of free and localized excitons from atomic monolayers in hybrid architectures *Optica* **4** 669–73
[29] He Y-M, Iff O, Lundt N, Baumann V, Davanco M, Srinivasan K, Höfling S and Schneider C 2016 Cascaded emission of single photons from the biexciton in monolayered WSe_2 *Nat. Commun.* **7** 13409

[30] Makhonin M N, Dixon J E, Coles R J, Royall B, Luxmoore I J, Clarke E, Hugues M, Skolnick M S and Fox A M 2014 Waveguide coupled resonance fluorescence from on-chip quantum emitter *Nano Lett.* **14** 6997–7002
[31] Zadeh I E, Elshaari A W, Jöns K D, Fognini A, Dalacu D, Poole P J, Reimer M E and Zwiller V 2016 Deterministic integration of single photon sources in silicon based photonic circuits *Nano Lett.* **16** 2289–94
[32] Tong L *et al* 2019 Artificial control of in-plane anisotropic photoelectricity in monolayer MoS_2 *Appl. Mater. Today* **15** 203–11
[33] Tütüncüoglu G, de La Mata M, Deiana D, Potts H, Matteini F, Arbiol J and Fontcuberta i Morral A 2015 Towards defect-free 1-D GaAs/AlGaAs heterostructures based on GaAs nanomembranes *Nanoscale* **7** 19453–60
[34] Yang Z, Surrente A, Tütüncüoglu G, Galkowski K, Cazaban-Carrazé M, Amaduzzi F, Leroux P, Maude D, Fontcuberta i Morral A and Plochocka P 2017 Revealing large-scale homogeneity and trace impurity sensitivity of GaAs nanoscale membranes *Nano Lett.* **17** 2979–84
[35] Friedl M *et al* 2018 Template-assisted scalable nanowire networks *Nano Lett.* **18** 2666–71
[36] Kim W, Güniat L, Fontcuberta i Morral A and Piazza V 2021 Doping challenges and pathways to industrial scalability of III–V nanowire arrays *Appl. Phys. Rev.* **8** 011304
[37] Dubrovskii V G, Kim W, Piazza V, Güniat L and Fontcuberta i Morral A 2021 Simultaneous selective area growth of wurtzite and zincblende self-catalyzed GaAs nanowires on silicon *Nano Lett.* **21** 3139–45
[38] Christopher J W, Vutukuru M, Lloyd D, Bunch J S, Goldberg B B, Bishop D J and Swan A K 2019 Monolayer MoS_2 strained to 1.3% with a microelectromechanical system *J. Microelectromech. Syst.* **28** 254–63
[39] Rojas-Lopez R R, Brant J C, Ramos M S O, Castro T H L G, Guimarães M H D, Neves B R A and Guimarães P S S 2021 Photoluminescence and charge transfer in the prototypical 2D/3D semiconductor heterostructure MoS_2/GaAs *Appl. Phys. Lett.* **119** 233101
[40] Lee C, Yan H, Brus L E, Heinz T F, Hone J and Ryu S 2010 Anomalous lattice vibrations of single-and few-layer MoS_2 *ACS Nano* **4** 2695–700
[41] Ávalos-Ovando O, Mastrogiuseppe D and Ulloa S E 2019 Lateral heterostructures and one-dimensional interfaces in 2D transition metal dichalcogenides *J. Phys.: Condens. Matter* **31** 213001
[42] Robert C *et al* 2016 Exciton radiative lifetime in transition metal dichalcogenide monolayers *Phys. Rev.* B **93** 205423
[43] Bayer M *et al* 2002 Fine structure of neutral and charged excitons in self-assembled In(Ga)As/(Al)GaAs quantum dots *Phys. Rev.* B **65** 195315
[44] Mitioglu A, Buhot J, Ballottin M, Anghel S, Sushkevich K, Kulyuk L and Christianen P 2018 Observation of bright exciton splitting in strained WSe_2 monolayers *Phys. Rev.* B **98** 235429
[45] Castellanos-Gomez A, Buscema M, Molenaar R, Singh V, Janssen L, Van Der Zant H S and Steele G A 2014 Deterministic transfer of two-dimensional materials by all-dry viscoelastic stamping *2D Mater.* **1** 011002